Correlation-Induced Sensitivity and Non-Hermitian Skin Effect of Quasiparticles

Tommaso Micallo,* Carl Lehmann, and Jan Carl Budich[†]

Institute of Theoretical Physics, Technische Universität Dresden and

Würzburg-Dresden Cluster of Excellence ct.qmat, 01062 Dresden, Germany

(Dated: February 2, 2023)

Non-Hermitian (NH) Hamiltonians have been shown to exhibit unique signatures, including the NH skin effect and an exponential spectral sensitivity with respect to boundary conditions. Here, we investigate as to what extent these remarkable phenomena, recently predicted and observed in a broad range of settings, may also occur in closed correlated fermionic systems that are governed by a Hermitian many-body Hamiltonian. There, an effectively NH quasiparticle description naturally arises in the Green's function formalism due to inter-particle scattering that represents an inherent source of dissipation. As a concrete platform we construct an extended interacting Su-Schrieffer-Heeger (SSH) model subject to varying boundary conditions, which we analyze using exact diagonalization and non-equilibrium Green's function methods. That way, we clearly identify the presence of the aforementioned NH phenomena in the quasi-particle properties of this Hermitian model system.

I. INTRODUCTION

Leveraging the concept of effective non-Hermitian (NH) Hamiltonians, a number of intriguing phenomena unique to dissipative systems have been recently experimentally discovered and explained with theory in a wide range of physical settings [1–12]. This prominently includes NH topological properties such as the winding of generalized energy eigenvalues in the complex plane [4, 13] entailing the NH skin effect, i.e., the accumulation of a macroscopic number of eigenstates at the boundary [14–19], as well as the anomalous sensitivity of surface zero-modes with respect to boundary conditions [6, 20–25].

In most physical scenarios, NH Hamiltonians are used as a conceptually simple tool to effectively model a system-environment coupling [10, 26], e.g. as an approximation to a quantum master equation. There, complex energy eigenvalues account for decay into a bath and the amplification from gain in an optically active system, respectively [10, 25, 27]. However, even in closed quantum many-body systems, quasi-particle excitations may exhibit effective dissipation due to their scattering off other degrees of freedom within the considered system [28–32]. The imaginary part of the quasi-particle energies, as described by the self-energy Σ entering the Green's function (GF), then models their lifetime, and non-trivial matrix structures of Σ have been found to give rise to interesting NH spectral properties such as exceptional points [33-39].

In this work, we study the NH boundary sensitivity of quasi-particles in a closed quantum many-body system, demonstrating the occurrence of both a NH skin effect and the striking sensitivity of a topological edge-mode with respect to small changes in the boundary conditions,

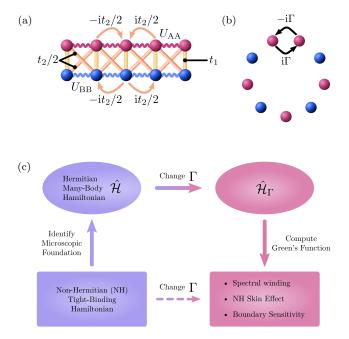


FIG. 1: (a) Illustration of the tight binding Hamiltonian \mathcal{H}_0 (Eq. (5)) with parameters t_1, t_2 and two-body interaction \mathcal{V} (Eq. (7)) with sublattice-specific interaction strenghts U_{AA}, U_{BB} in a two-leg ladder geometry, with sublattice A (B) as the red upper (blue lower) leg. (b) Illustration of the broken ring geometry with generalized boundary condition parametr $\Gamma \in [0, 1]$, where $\Gamma = 0$ ($\Gamma = 1$) corresponds to open (periodic) boundary conditions. (c) Schematic illustration of solid arrows is followed to demonstrate its (qualitative) commutation with the beaten dashed path.

despite the Hermitian nature of the governing many-body Hamiltonian. To this end, we construct and solve a model for a one-dimensional chain of correlated fermions with sub-lattice dependent interactions and varying boundary conditions (see Fig. 1(a-b) for an illustration) at finite temperature. In the framework of full exact diagonalization (ED), we extract the NH quasi-particle Hamiltonian

^{*}Electronic address: tommaso.micallo@tu-dresden.de

[†]Electronic address: jan.budich@tu-dresden.de

directly from the Källén-Lehmann representation of the retarded GF, and analyze its NH skin effect. In addition, to access bigger system sizes, we compute the GF within the conserving second Born approximation (SBA), thus finding numerical evidence for a sensitivity of the lowest lying quasi-particle mode with respect to boundary conditions that scales exponentially in system size. Our results corroborate the picture that quasi-particles behave qualitatively similarly to excitations of an effective NH tight-binding model, even when it comes to changes in the boundary conditions of the underlying many-body Hamiltonian (cf. commuting diagram in Fig. 1(c)), which implies genuinely NH spectral and spatial distribution properties [25, 38, 40, 41].

The remainder of this article is structured as follows: The Green's function formalism underlying the definition of an effective NH quasi-particle Hamiltonian is discussed in Section II A, together with a brief synopsis of the numerical methods used to compute the GF. In Section II B, a microscopic model is constructed so as to mimic a topological NH tight-binding model at the quasi-particle level. This model is analyzed in Section III, demonstrating how the effective NH Hamiltonian responds to varying boundary conditions of the many-body Hamiltonian. A concluding discussion is presented in Section IV. In this work, we use the natural units $\hbar = k_{\rm B} = 1$.

II. METHODS AND MODEL BUILDING

A. From Green's functions to Non-Hermitian Hamiltonians

In correlated quantum many-body systems, many important physical aspects such as response properties and elementary excitations are encoded in correlation functions [42]. In particular, equilibrium quasi-particle properties including the spectral functions and key susceptibilities are described by the single-particle (or two-point) retarded Green's function (rGF). In this framework, the notion of an independent particle described by a non-interacting Hermitian Hamiltonian may be replaced by a quasi-particle governed by and effective NH Hamiltonian $\mathcal{H}_{\text{eff}}[28, 32, 37, 38, 41, 43]$. There, the NH character reflects the finite lifetime of quasi-particles due to inter-particle scattering [43]. In the real-space and time domain, the rGF is defined as

$$G_{m,n}^{\mathrm{R}}(t) = -\mathrm{i}\theta(t)\left\langle \left\{ c_m(0), c_n^{\dagger}(t) \right\} \right\rangle, \qquad (1)$$

where c(t), $(c^{\dagger}(t'))$ is the annihilation (creation) operator in the Heisenberg picture, m, n are indices referring to both spatial and internal (e.g. sublattice) degrees of freedom, and $\langle ... \rangle$ is the thermal average with respect to the full many-body Hamiltonian \mathcal{H} . Fourier transforming to the frequency domain with respect to t, the frequency-dependent effective NH Hamiltonian $\mathcal{H}_{\text{eff}}(\omega)$ and self energy $\Sigma(\omega)$ are introduced as

$$G^{\mathrm{R}}(\omega) = \lim_{\eta \to 0^{+}} (\omega + \mathrm{i}\eta - \mathcal{H}_{\mathrm{eff}}(\omega))^{-1} ; \qquad (2)$$

$$\mathcal{H}_{\text{eff}}(\omega) = \mathcal{H}_0 + \Sigma(\omega), \qquad (3)$$

where matrix indices have been dropped for brevity. We focus on quasi-particle excitations close to the Fermi energy ($\omega = 0$) and their NH topological properties. To obtain a frequency independent effective NH Hamiltonian, we approximate the self energy by its value $\Sigma = \Sigma(0)$ at the Fermi energy. Generally speaking, since the poles of the rGF (see Eq. (2)) lie in the lower half of the complex plane, the eigenvalues of \mathcal{H}_{eff} can only have nonpositive imaginary parts, corresponding to negative inverse of lifetimes. We now outline how the rGF is practically computed in our present analysis.

Exact Diagonalization. For finite chains of modest size, the many-body Hamiltonian $\mathcal{H} = \mathcal{H}_0 + \mathcal{V}$ with noninteracting part \mathcal{H}_0 and interaction potential \mathcal{V} can be fully diagonalized by solving $\mathcal{H} | E_{\mu} \rangle = E_{\mu} | E_{\mu} \rangle$. Then, the rGF can be computed within the Källén-Lehmann representation[44] as

$$G_{m,n}(\omega) =_{\eta \to 0^{+}} \sum_{\mu,\nu} \frac{\mathrm{e}^{-E_{\mu}/T}}{Z} \times \left[\frac{\langle E_{\mu} | c_{m} | E_{\nu} \rangle \langle E_{\nu} | c_{n}^{\dagger} | E_{\mu} \rangle}{\omega + \mathrm{i}\eta + E_{\mu} - E_{\nu}} + \frac{\langle E_{\nu} | c_{m} | E_{\mu} \rangle \langle E_{\mu} | c_{n}^{\dagger} | E_{\nu} \rangle}{\omega + \mathrm{i}\eta + E_{\nu} - E_{\mu}} \right].$$

$$(4)$$

Numerically, the limit $\eta \to 0^+$ of the regularization parameter must be approximated, thus setting a limit to the resolution in frequency (or energy). While conferring to the finite size rGF a characteristic spiky spectral structure, the choice of a small but finite regularization parameter only affects quantitatively, but not qualitatively the results presented in this work. To retrieve the effective Hamiltonian (3), the limit $\eta \to 0$ is withheld, and effectively frequency is treated as a complex parameter with a small but finite imaginary part. Where ED results are shown, we use $\eta = 0.015$.

Second Born approximation. To access longer chains we use the non-equilibrium Green's function approach in conserving second Born approximation (SBA) [45-49], where the limiting factor is that only chains with weak to moderate interaction strengths can be solved to satisfactory accuracy [49, 50]. In this framework, we numerically compute the equilibrium rGF in real time (see Eq. (1)) by solving the Kadanoff-Baym equations of motion, building on the software package NESSi [49]. For sufficiently long times, the amplitude of the rGF is damped by the interaction induced dissipation, thus allowing us to converge the Fourier transform to frequency space in order to extract the effective NH Hamiltonian (3).

B. Microscopic lattice model

We now construct a microscopic model for a Hermitian many-body Hamiltonian \mathcal{H} that yields a topologically nontrivial quasi-particle spectrum at the effective NH Hamiltonian level (see Eq. (3)). In particular, we find it interesting to investigate whether quasiparticles can exhibit a similarly dramatic response to changes in the boundary conditions of \mathcal{H} as excitations in NH topological tight-binding models are known to exhibit. To this end we proceed in two steps. First, we discuss an effective NH tight-binding model that has the conceptually simplest anti-Hermitian part enabling the aforementioned NH topological features. The Hermitian part of this NH toy model is then adopted as the non-interacting part \mathcal{H}_0 of our microscopic model. Second, a two-body scattering term \mathcal{V} is constructed that may induce a self-energy mimicking the anti-Hermitian part of the toy model. This results in the full Hermitian Hamiltonian $\mathcal{H} = \mathcal{H}_0 + \mathcal{V}$.

Target NH tight binding model. To set the stage, we briefly discuss a NH generalization of the celebrated Su-Schrieffer-Heeger (SSH) model [24, 51, 52] as an archetype of a topological NH tight-binding model that we aim at mimicking further below with the quasiparticle excitations of a Hermitian many-body model. The Hermitian part of the Hamiltonian is given by

$$\mathcal{H}_0 = \sum_j t_1 c_j^{\dagger} \sigma_x c_j + \sum_j \frac{t_2}{2} c_j^{\dagger} (\sigma_x + \mathrm{i}\sigma_z) c_{j+1} + \mathrm{H.c.}, \quad (5)$$

where $c_j = (c_{j,\mathrm{A}}, c_{j,\mathrm{B}})^T$ is the annihilation operator in unit cell j, which has a two-spinor structure in A-B-sublattice space, where the standard Pauli matrices σ_x, σ_z act.

The anti-Hermitian part is assumed to be of the form

$$\mathcal{H}_{\rm AH} = -i \sum_{j} c_{j}^{\dagger} \left(\gamma_{z} \sigma_{z} - \gamma_{0} \sigma_{0} \right) c_{j}, \tag{6}$$

where $\gamma_0, \gamma_z \geq 0$ and the causality constraints of the rGF amount to $\gamma_0 \geq \gamma_z$. Even though the γ_0 -term is a simple vertical shift of the eigenenergies in the complex plane, it is thus of fundamental importance for the physical interpretation in terms of quasi-particles with a finite lifetime. For $\gamma_z \neq 0$, the system exhibits topologically nontrivial properties including a spectral winding around the base point $E_{\rm b} = -i\gamma_0$ for periodic boundary conditions (PBC)[4, 52], the NH skin effect for open boundary conditions (OBC) [40], and an exponential sensitivity of a spectrally isolated mode with respect to boundary conditions [24]. We will discuss these intriguing phenomena in more detail when analyzing their occurrence one by one in the quasi-particle spectrum of our microscopic model in Sec. III.

Sublattice dependent interaction. From Eq. (6), we note that the anti-Hermitian part of our targeted NH tight-binding model is diagonal in real space. While \mathcal{H}_{AH} is independent of the unit cell (translation invariance), it does depend on sub-lattice for finite γ_z , i.e. in any topologically non-trivial scenario. Quite intuitively, a contribution of this form to the self-energy may emerge from a sub-lattice dependent interaction potential, which physically corresponds to different scattering rates within particles on A sites as compared to particles on B sites, and thus a sublattice-dependent quasi-particle life-time [37, 39]. While momentum-transfer in scattering processes may give rise to a more complicated momentumdependent profile of the scattering rates, the local selfenergy is still expected to have the largest magnitude in a finite temperature system. Guided by this intuition, in the following we solve a microscopic many-body model defined by adding to the free Hermitian Hamiltonian \mathcal{H}_0 (see Eq. (5)) the sublattice dependent two-body interaction

$$\mathcal{V} = \sum_{\alpha} \sum_{j} U_{\alpha\alpha} \left(n_{j,\alpha} - \frac{1}{2} \right) \left(n_{j+1,\alpha} - \frac{1}{2} \right), \quad (7)$$

where $\alpha = A, B$ and $n_{j,\alpha} = c_{j,\alpha}^{\dagger} c_{j,\alpha}$ denotes the number operator on sublattice α in unit cell j. Without loss of generality, in the following we assume $U_{AA} > U_{BB}$ to induce a staggered scattering rate corresponding to a finite γ_z in Eq. (6). Our full model described by the Hamiltonian $\mathcal{H} = \mathcal{H}_0 + \mathcal{V}$ is illustrated in Fig. 1(a). This model preserves the unitary particle-hole symmetry C, i.e. $C\mathcal{H}C^{-1} = \mathcal{H}$ which is defined by its action

$$Cc_{i,A}C^{-1} = -c_{i,A}^{\dagger}, \quad Cc_{i,B}C^{-1} = c_{i,B}^{\dagger}$$
(8)

on the field operators and along with its linearity[53]. Note that this symmetry also imposes constraints on the the quasiparticle spectra via the self-energy, as will be discussed in Sec. III (cf. Eq. (10 - 11)).

III. NUMERICAL RESULTS FOR GENERALIZED BOUNDARY CONDITIONS

We now discuss our numerical results for the rGF of the model described by $\mathcal{H} = \mathcal{H}_0 + \mathcal{V}$ (see Eq. (5) and Eq. (7)) obtained in the framework of full exact diagonalization and conserving second Born approximation. respectively (cf. Sec. II A). Our goal is to analyze as to what extent intriguing NH topological phenomena hosted by the NH tight binding model $\mathcal{H}_0 + \mathcal{H}_{AH}$ (see Eq. (5) and Eq. (6) can be found in the quasi-particle behavior (as governed by Eq. (3)) of our microscopic manybody model. Specifically, solving for the rGF at finite temperature T and with generalized boundary conditions $\Gamma \in [0, 1]$ (see Fig. 1b), we will study the following three related properties: The spectral winding of complex quasi-particle energies (Sec. III A), the non-Hermitian skin effect (Sec. IIIB), and the exponentially enhanced sensitivity of a spectrally isolated mode (Sec. III C).

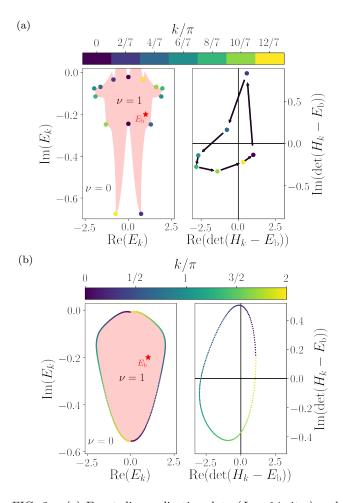


FIG. 2: (a) Exact diagonalization data (L = 14 sites) and (b) Second Born Approximation data (L = 400 sites) for effective NH Hamiltonians under periodic boundary conditions (PBC). Left panels: complex spectra with PBC showing a point gap, reference point $E_{\rm b} = 1 - 0.2$ i denoted as a red star; the red shaded area contains all the reference point, where formally $\nu = 1$ holds. Right panels: corresponding nontrivial winding of the determinant around the origin, following equation (9), with reference point $E_{\rm b} = 1 - 0.2$ i. Data obtained for $t_2 = -t_1 = 1$, $U_{AA} = 1.5$, $U_{BB} = 0.1$, T = 5. The arrows and the colors in the right panels show in both cases a counterclockwise winding corresponding to $\nu = 1$.

A. Spectral Winding

We start by considering a translation-invariant system with PBC, such that lattice momentum k is a good quantum number of \mathcal{H}_{eff} . In this scenario, a topologically non-trivial quasi-particle spectrum is characterized by the winding number [4]

$$\nu = \oint_{-\pi}^{\pi} \frac{\mathrm{d}k}{2\pi \mathrm{i}} \partial_k \log \, \det \left[\mathcal{H}_{\mathrm{eff}}(k) - E_{\mathrm{b}}\right] \tag{9}$$

around a fixed base point $E_{\rm b}$ in the complex energy plane. A non-vanishing ν in system with PBC has been identified as a prerequisite for the NH skin

effect [17] and the exponentially enhanced boundary sensitivity [24] to be investigated further below. For finite systems with L unit cells, we compute ν using a straightforward discretized version of Eq. (9), i.e $\nu = \frac{1}{2\pi} \sum_n (\arg \det [\mathcal{H}_{\text{eff}}(k_{n+1}) - E_{\text{ref}}]$ arg det $[\mathcal{H}_{\text{eff}}(k_n) - E_{\text{ref}}]$) with $k_n = 2\pi n/L$; n = $0, 1, \ldots, L - 1$. We note that \mathcal{H}_{eff} inherits the particlehole symmetry of \mathcal{H} (cf. Eq. (8)). Specifically, from the basic definition of the rGF as a correlation function of field operators (see Eq. (1)), the particle-hole symmetry (8) can be shown to act on the effective NH $\mathcal{H}_{\text{eff}}(k)$ as [54–56]

$$\sigma_z \mathcal{H}_{\text{eff}}(k) \sigma_z = -\mathcal{H}^*_{\text{eff}}(-k) \tag{10}$$

which has the immediate implication

$$\{E_k\} \stackrel{\text{PH}}{\longleftrightarrow} \{-E_{-k}^*\}.$$
 (11)

on the complex energy eigenvalues, i.e. the imaginary axis is a symmetry axis of the spectrum. This behavior is confirmed by our numerical data (see the left panel in Fig. 2a for ED and Fig. 2b for SBA data, respectively). These spectra also show a clear point gap that we characterize via the associated winding number. This NH topological signature highlighted in the corresponding right panels, showing how a phase is accumulated when following equation (9). While only the larger system sizes treated within SBA render the spectrum a smooth curve in the complex plane, the ED data clearly indicates a qualitatively similar winding behavior already in small systems of L = 14 sites. From this data, we are able to conclude that, while the self energies obtained with both methods contain additional k-dependent terms beyond the simple ansatz in Eq. (6), the basic intuition of a local self-energy modeled by a finite γ_z is sufficient to correctly anticipate the topological winding protected by a point gap.

B. Non-Hermitian Skin Effect

For NH Hamiltonians with $\nu \neq 0$ at PBC, it is well known that the spectrum for OBC may completely change its topology, so as to assume an open arc shape in the complex energy plane that is localized inside the loop defined by the PBC spectrum [17, 57]. Moreover, at OBC a macroscopic number of right eigenstates may localize at one end of the chain, while the corresponding left eigenstates will localize at the opposite end [40]. This is the so-called NH skin effect, the counterpart of $\nu \neq 0$ under OBC [17, 57]. While these phenomena have been found and explained with theory in the context of a generalized bulk-boundary correspondence (GBBC) in many NH tight-binding models (see Ref. [40] for an overview), here we investigate their occurrence from fully microscopic principles in the effective NH Hamiltonian derived from the rGF of a correlated Hermitian many-body model. In other words, in our analysis the boundary conditions are

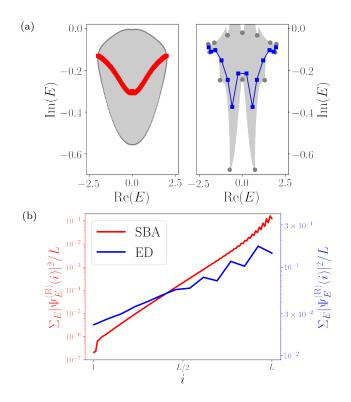


FIG. 3: (a) Spectral collapse under open boundary conditions (OBC) for SBA data (red, L = 100 sites) and ED data (blue, L = 14 sites), respectively, shown on top of the corresponding PBC data (grey). The spectra drastically change to an arc-shape inside the shaded area associated with $\nu = 1$. (b) Exponential localization of the total spectral weight of right eigenstates as a function of the site index, exemplifying the NH skin effect for SBA data (red, L = 100 sites) and ED data (blue, L = 14 sites). Data obtained for $t_2 = -t_1 = 1$, $U_{AA} = 1.5$, $U_{BB} = 0.1$, T = 5.

not modified at the level of a NH single-particle Hamiltonian but at the microscopic level of the Hermitian manybody Hamiltonian \mathcal{H} . We stress that also for OBC, the particle hole symmetry of \mathcal{H} imposes the symmetry $\{E\} \stackrel{\text{PH}}{\longleftrightarrow} \{-E^*\}$ on the complex spectrum of \mathcal{H}_{eff} . In our effective model, using the same parameters and methods as in the previous section on PBC, in Fig. 3 we observe both the effect of OBC on the complex energy levels collapsing to an arc-shape and demonstrate the occurrence of a NH skin effect for the eigenstates of the effective NH Hamiltonian. Even though this behavior is compatible with intuition about the GBBC occurring in NH tightbinding models, we find it remarkable how the effect of OBC applied to the Hermitian many-body Hamiltonian \mathcal{H} indeed manifests in the quasi-particle properties according to the principles of NH topology. Again, the computed OBC self-energies quantitatively deviate from the simple toy model in Eq. (6) so as to include nonlocal terms, but the presence of these additional perturbations is not capable of changing the qualitative topological change of the spectrum. The skin effect and the stark change in the eigenvalues when the boundary con-

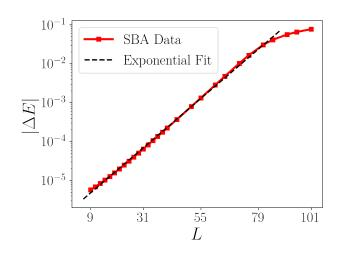


FIG. 4: Shift ΔE of the generalized imaginary zero-mode E_{Γ} as a function of the number of sites L as a consequence of the activation of the end-to-end hopping $\Gamma = 10^{-5}$ (see Eq. (13)). An exponential fit (dashed line) closely matching our numerical data is plotted as a guide to the eye. The fit excludes the last three point at L = 91,95,101, where the exponential behavior crosses over to a saturated regime. Data obtained via SBA for $t_2 = -t_1 = 1$, $U_{AA} = 1.5$, $U_{BB} = 0.1$, T = 5.

ditions are varied are key ingredients for the exponential sensitivity analyzed in the following subsection.

C. Exponential Sensitivity

We now turn to considering our model at generalized boundary conditions (GBC) that are used to bridge continuously between open ($\Gamma = 0$) and closed ($\Gamma = 1$) boundary conditions. For systems exhibiting a non-zero spectral winding number ν , an exponential sensitivity in system size of an isolated mode within the point gap has been predicted [24]. Given that the quasi-particle spectrum of our model system exhibits both $\nu \neq 0$ and the NH skin effect, we find it interesting to study whether even this exponential sensitivity with respect to small changes of Γ can be identified in our present context.

As shown in Fig. 1b, the system under consideration here has an odd number of sites. Since the Hermitian end-connecting term

$$\mathcal{H}_{0,\text{ends}} = i\Gamma c_{N,A}^{\dagger} c_{0,A} + \text{h.c.}$$
(12)

 $(\Gamma \in \mathbb{R})$ preserves the PH symmetry, the spectrum of \mathcal{H}_{eff} is symmetric around the imaginary axis, implying that at least one eigenvalue of \mathcal{H}_{eff} must be purely imaginary, independently of the system size. No symmetry-preserving perturbation or interaction can unpin this mode from the imaginary axis, similarly to how a chiral-protected zero mode must always exist in a Hermitian SSH mode with an odd number of sites. This generalized imaginary zero-mode solves the eigenproblem $\mathcal{H}_{\text{eff}}(\Gamma) |0\rangle = -iE_{\Gamma} |0\rangle$ with $E_{\Gamma} > 0$. Adapting the analysis in Ref. [24] to this

scenario, the spectrally isolated eigenvalue is predicted to shift in response to a change in Γ as

$$|\Delta E| = |E_{\Gamma} - E_0| = \Delta_0 e^{\alpha L}, \qquad (13)$$

where $\alpha > 0$, i.e. an enhanced sensitivity with increasing system size, is expected for $\nu \neq 0$, while at $\nu = 0$ and the absence of the NH skin effect, $\alpha < 0$ represents an exponential damping of the level shift.

To clearly identify an exponential scaling, system sizes beyond the scope of full ED are necessary, which is why the data in this section is exclusively based on SBA. Quite remarkably, the effective Hamiltonian computed within SBA clearly exhibits the exponential sensitivity described by Eq. (13) (see Fig. 4). More specifically, the level shift increases exponentially in systems size over more than three orders of magnitude, before leveling off at a value that is comparable to the size of the point gap of the system along the imaginary axis. This is a strong piece of evidence that topological principles unique to NH systems can manifest in the quasiparticles of many-body systems governed at the microscopic level by a Hermitian Hamiltonian. Similar to the cases on OBC and PBC, the effects on the self-energy of changing Γ at GBC are richer than in previously considered NH tight-binding toy models. However, the qualitative similarity of our microscopic results to a simple toy model using the NH term (6) highlights the topological robustness of the studied phenomena.

IV. CONCLUSIONS

In summary, we have designed and studied a Hermitian one-dimensional many-body system of correlated fermions, whose quasiparticle description mimics a topologically non-trivial NH tight-binding model. Specifically, we have investigated several boundary-dependent properties that, at the single-particle level, are unique to NH systems. That way we have demonstrated how changing the boundary conditions of the Hermitian many-body Hamiltonian can indeed have a similar effect on the quasi-particle properties as directly changing the boundary conditions in an effective NH tight-binding model, at least as far as NH topological properties are concerned. In the schematic language of Fig. 1c, we have shown that the dashed and the solid path of the diagram qualitatively commute.

Our findings give a fully microscopic physical basis in the realm of quantum many-body physics to several intriguing NH topological phenomena that have been predicted at the level of effective NH single-particle models, including the NH skin effect and the exponential sensitivity of a spectrally isolated edge mode with respect to small changes in the boundary conditions. These general insights suggest that experimental signatures of NH topology can be found in basic spectroscopic experiments and quantum transport settings, the closer analysis of which defines an interesting direction of future work.

Acknowledgments

We would like to thank Lorenzo Crippa, Benjamin Michen, and Alessandro Santini (TM) for discussions. We acknowledge financial support from the German Research Foundation (DFG) through the Collaborative Research Centre SFB 1143 (Project No. 247310070), the Cluster of Excellence ct.qmat (Project No. 390858490), and the DFG Project 419241108. Our numerical calculations were performed on resources at the TU Dresden Center for Information Services and High Performance Computing (ZIH).

- M. S. Rudner and L. S. Levitov, Physical Review Letters 102 (2009).
- [2] J. M. Zeuner, M. C. Rechtsman, Y. Plotnik, Y. Lumer, S. Nolte, M. S. Rudner, M. Segev, and A. Szameit, Physical Review Letters 115 (2015).
- [3] T. E. Lee, Physical Review Letters **116** (2016).
- [4] Z. Gong, Y. Ashida, K. Kawabata, K. Takasan, S. Higashikawa, and M. Ueda, Physical Review X 8 (2018).
- [5] H. Zhou, C. Peng, Y. Yoon, C. W. Hsu, K. A. Nelson, L. Fu, J. D. Joannopoulos, M. Soljačić, and B. Zhen, Science **359**, 1009 (2018).
- [6] F. K. Kunst, E. Edvardsson, J. C. Budich, and E. J. Bergholtz, Physical Review Letters 121 (2018).
- [7] S. Imhof, C. Berger, F. Bayer, J. Brehm, L. W. Molenkamp, T. Kiessling, F. Schindler, C. H. Lee, M. Greiter, T. Neupert, and R. Thomale, Nature Physics 14, 925 (2018).

- [8] S. Yao, F. Song, and Z. Wang, Physical Review Letters 121 (2018).
- [9] L. Xiao, T. Deng, K. Wang, G. Zhu, Z. Wang, W. Yi, and P. Xue, Nature Physics 16, 761 (2020).
- [10] Y. Ashida, Z. Gong, and M. Ueda, Advances in Physics 69, 249 (2020).
- [11] S. Weidemann, M. Kremer, T. Helbig, T. Hofmann, A. Stegmaier, M. Greiter, R. Thomale, and A. Szameit, Science 368, 311 (2020).
- [12] C. Yuce, Annals of Physics **415**, 168098 (2020).
- [13] H. Shen, B. Zhen, and L. Fu, Physical Review Letters 120 (2018).
- [14] S. Yao and Z. Wang, Physical Review Letters 121 (2018).
- [15] C. H. Lee and R. Thomale, Physical Review B 99 (2019).
- [16] D. S. Borgnia, A. J. Kruchkov, and R.-J. Slager, Physical Review Letters 124 (2020).
- [17] N. Okuma, K. Kawabata, K. Shiozaki, and M. Sato,

Physical Review Letters 124 (2020).

- [18] T. Helbig, T. Hofmann, S. Imhof, M. Abdelghany, T. Kiessling, L. W. Molenkamp, C. H. Lee, A. Szameit, M. Greiter, and R. Thomale, Nature Physics 16, 747 (2020).
- [19] M. Žnidarič, Phys. Rev. Res. 4, 033041 (2022).
- [20] Y. Xiong, Journal of Physics Communications 2, 035043 (2018).
- [21] N. Okuma and M. Sato, Physical Review Letters 123 (2019).
- [22] L. Li, C. H. Lee, S. Mu, and J. Gong, Nature Communications 11 (2020).
- [23] R. Koch and J. C. Budich, The European Physical Journal D 74 (2020).
- [24] J. C. Budich and E. J. Bergholtz, Physical Review Letters 125 (2020).
- [25] F. Koch and J. C. Budich, Physical Review Research 4 (2022).
- [26] T. Fukui and N. Kawakami, Physical Review B 58, 16051 (1998).
- [27] H. Menke and M. M. Hirschmann, Physical Review B 95 (2017).
- [28] L. P. Pitaevskii and E. M. Lifshitz, *Statistical Physics*, Part 2 (Butterworth-Heinemann, Woburn, MA, 1980).
- [29] I. Rotter, Journal of Physics A: Mathematical and Theoretical 42, 153001 (2009).
- [30] A. A. Zyuzin and A. Y. Zyuzin, Physical Review B 97 (2018).
- [31] Y. Michishita and R. Peters, Physical Review Letters 124 (2020).
- [32] N. Okuma and M. Sato, Physical Review Letters 126 (2021).
- [33] M. Berry, Czechoslovak Journal of Physics 54, 1039 (2004).
- [34] T. Yoshida, R. Peters, and N. Kawakami, Physical Review B 98 (2018).
- [35] T. Yoshida, R. Peters, N. Kawakami, and Y. Hatsugai, Progress of Theoretical and Experimental Physics 2020 (2020).
- [36] Y. Nagai, Y. Qi, H. Isobe, V. Kozii, and L. Fu, Physical Review Letters 125 (2020).
- [37] R. Rausch, R. Peters, and T. Yoshida, New Journal of Physics 23, 013011 (2021).

- [38] B. Michen, T. Micallo, and J. C. Budich, Physical Review B 104 (2021).
- [39] C. Lehmann, M. Schüler, and J. C. Budich, Physical Review Letters 127 (2021).
- [40] E. J. Bergholtz, J. C. Budich, and F. K. Kunst, Reviews of Modern Physics 93 (2021).
- [41] L. Crippa, J. C. Budich, and G. Sangiovanni, Physical Review B 104 (2021).
- [42] A. Zagoskin, Quantum Theory of Many-Body Systems (Springer International Publishing, 2014).
- [43] V. Kozii and L. Fu, "Non-hermitian topological theory of finite-lifetime quasiparticles: Prediction of bulk fermi arc due to exceptional point," (2017).
- [44] Z. Wang and S.-C. Zhang, Physical Review X 2 (2012).
- [45] G. Stefanucci and R. van Leeuwen, *Nonequilibrium Many-Body Theory of Quantum Systems* (Cambridge University Press, 2013).
- [46] K. Balzer and M. Bonitz, Nonequilibrium Green's Functions Approach to Inhomogeneous Systems (Springer Berlin Heidelberg, 2013).
- [47] H. Aoki, N. Tsuji, M. Eckstein, M. Kollar, T. Oka, and P. Werner, Reviews of Modern Physics 86, 779 (2014).
- [48] N. Schlünzen and M. Bonitz, Contributions to Plasma Physics 56, 5 (2016).
- [49] M. Schüler, D. Golež, Y. Murakami, N. Bittner, A. Herrmann, H. U. Strand, P. Werner, and M. Eckstein, Computer Physics Communications 257, 107484 (2020).
- [50] Y. Murakami, M. Schüler, S. Takayoshi, and P. Werner, Physical Review B 101 (2020).
- [51] W. P. Su, J. R. Schrieffer, and A. J. Heeger, Physical Review Letters 42, 1698 (1979).
- [52] S. Lieu, Physical Review B 97 (2018).
- [53] S. Ryu, A. P. Schnyder, A. Furusaki, and A. W. W. Ludwig, New Journal of Physics 12, 065010 (2010).
- [54] C.-K. Chiu, J. C. Teo, A. P. Schnyder, and S. Ryu, Reviews of Modern Physics 88 (2016).
- [55] K. Kawabata, K. Shiozaki, M. Ueda, and M. Sato, Physical Review X ${\bf 9},$ 041015 (2019), 1812.09133 .
- [56] N. Okuma, Physical Review B **105** (2022).
- [57] K. Zhang, Z. Yang, and C. Fang, Physical Review Letters 125 (2020).